

Fermi Level Equilibration in Quantum Dot–Metal Nanojunctions[†]Annabel Wood,[‡] Michael Giersig,[§] and Paul Mulvaney^{*,‡,||}

School of Chemistry, University of Melbourne, Parkville, Victoria 3010, Australia, Hahn-Meitner Institut, Department Solar Energy Research, Glienickestr.100, Berlin, 14109, Germany, and Max-Planck Institute for Colloids and Surfaces, Potsdam-Golm, 14476, Germany

Received: April 26, 2001

The process of Fermi level equilibration in 5 nm ZnO quantum dot–metal nanojunctions has been monitored using changes to both the surface plasmon band of the metal island and the sharp exciton band of the ZnO nanocrystals following photoinduced electron accumulation. In the cases of silver, copper, and gold islands, excess electrons reside on both the quantum dot and the metal, whereas for Pt islands, the excess electrons reside exclusively on the Pt island. Electrons are transferred rapidly from Pt to the solvent ethanol, preventing accumulation on the quantum dots. The combination of exciton bleaching and surface plasmon shifts provides a simple way of probing the efficiency of small metal islands as redox catalysts on semiconductor particles.

Introduction

One of the fundamental challenges in quantum dot chemistry is unravelling the various relaxation processes that occur following the creation of electron–hole pairs or excitons within the semiconductor particle. Generally, one is interested in two extreme cases. In the first, maximum band edge luminescence is desired; that is, all charge carriers should recombine radiatively, and no redox reactions should occur at the surface. At the other extreme, one wants to extract chemical energy out of the illuminated particle, by maximizing electron–hole separation. In artificial photosynthesis and photochemical energy storage schemes, rapid, quantitative transfer of one of the charge carriers to a solution-phase redox couple is then usually required. One of the most common methods for facilitating electron transfer from conduction band electrons to solution species has been through the use of metal island catalysts deposited onto the quantum dot (QD) surface. These metal islands mediate multielectron redox processes with solution phase redox carriers, and enhancements of both anodic and cathodic redox processes have been observed at illuminated semiconductor electrodes that have metal island deposits.^{1–8}

For macroscopic *n*-type materials in contact with metals a Schottky barrier (depletion layer) normally forms at the junction between the two materials, which reduces the kinetics of electron injection from the semiconductor conduction band into the metal. Curran and Lamouche⁷ pointed out that because the diameter of a QD is significantly smaller than that of the depletion layer, there is no significant depletion layer within the QD to impede electron transfer. Gerischer⁸ subsequently suggested that, for hydrogen loaded metal islands at least, an accumulation layer may in fact be created, which could accelerate electron transfer to the metal island from the QD. Although it is not clear what type of electronic barrier exists between the QD and metal island, Grätzel¹ noted that free diffusion of charge carriers alone will permit electron transfer within a time $R^2/\pi^2 D \approx 0.1$ ps to

a metal island or adsorbed electron acceptor (for an electron diffusion coefficient of ~ 0.1 cm² s⁻¹), which is rapid enough to compete with recombination processes.^{10–12}

The question we were interested in probing was whether photoelectrons in fact migrate efficiently to metal island catalysts on an *n*-type semiconductor particle surface or whether some electrons accumulate on the semiconductor. If excess electrons remain on the semiconductor, then subsequent electron–hole charge separation is likely to be very inefficient due to rapid reaction of the nascent holes with the resident excess electrons in the *n*-type material. However, to identify where the charges reside at equilibrium, we need to be able to spectrophotometrically monitor electrons on both sides of the junction separately.

One way to determine the presence of excess charge on the QD is through exciton bleaching. For semiconductors with strong exciton absorption bands in the visible part of the spectrum such as ZnO, it is well established that excess electrons^{13,14} induce a dramatic bleaching of the exciton band. This is attributed to either the Mosse–Burstein effect (band filling¹⁵), or to electric field modulated effects on the excitonic levels by trapped carriers, the so-called Stark effect.^{16,17} Unfortunately, while titanium dioxide is the most commonly used and efficient UV photocatalyst in use at present, its solid-state properties are not particularly useful for such studies. Its absorption spectrum is largely featureless, and excess photoelectrons within the conduction band can only be observed from the very weak blue color of the trapped electrons.^{1,18} Conversely, ZnO is a photocatalytically active metal oxide, which exhibits strong exciton absorption. It is also well-known that the exciton absorption bands of both ZnO colloids and ZnO nanoparticle films^{11,19,20} are strongly bleached by the presence of accumulated conduction band electrons. This provides a simple optical method for determining the presence of excess electrons on the ZnO QDs.

Small metal islands of Ag, Au, and Cu can be deposited onto the ZnO surface photochemically. If the metal islands are small enough, then their characteristic surface plasmon bands will be observed in the ZnO–metal absorption spectrum. The position of the surface plasmon band position depends on the conduction band electron density.²¹ Increases in electron density cause a

[†] Part of the special issue “Royce W. Murray Festschrift”.

* Corresponding author. Email: mulvaney@unimelb.edu.au.

[‡] University of Melbourne.

[§] Hahn-Meitner Institut.

^{||} Max-Planck Institute for Colloids and Surfaces.

blue shift in the band position. The changes in band position can then be used to see whether the metal islands accumulate charge efficiently from the illuminated semiconductor particles.

By combining both of these optical effects, it becomes possible to see where the photoelectrons reside in an illuminated quantum dot–metal nanojunction. The aim of this paper is thus to demonstrate the equilibration of the quasi-Fermi level of an illuminated quantum dot with the Fermi level of a contacted metal island catalyst particle and to compare this process for different metal catalysts. We will show that it is possible to readily distinguish between the different metals as redox catalysts, even through the use of quasi-steady-state photolysis experiments.

Experimental Section

To prepare ZnO QDs (Q-ZnO), 100 mL of 20 mM analytical grade zinc acetate dihydrate (Aldrich) dissolved in pure, dry ethanol was placed in an Erlenmeyer flask equipped with a septum and vigorously stirred. A 1.7 mL sample of tetramethylammonium hydroxide (TMAOH) (25 wt % in methanol from Aldrich) was added at a rate of 100 $\mu\text{L}/\text{min}$, using a motor-driven syringe to ensure continuous, reproducible addition. The size of the quantum dots could be varied by heating or cooling the zinc acetate solution to a desired temperature before addition of TMAOH. For the experiments described here, a synthesis temperature of 60 $^{\circ}\text{C}$ was used, which yielded Q-ZnO with a mean diameter of approximately 5 nm. This procedure represents an enormous simplification over the currently employed synthesis, first described by Spanhel and Anderson,²² and yields at -5°C the smallest Q-ZnO to date, with an exciton peak at 270 nm. A medium-pressure mercury lamp (Bausch and Lomb) was used as the excitation source in the photolysis experiments. The lamp was fitted with a heat absorbing filter (Oriol #6127) and a broad band-pass filter (Oriol #59152) so that only UV light between 200 and 400 nm entered the photolysis cells. A 5 mL sample of ZnO QDs was placed in a 1 cm path length quartz cuvette, and ethanol or metal salts were added to bring the total solution volume to 5.5 mL, with a Q-ZnO concentration of ~ 0.9 mM and a metal ion concentration of 25–250 μM . The cell was fitted either with a fine capillary bubbler or a vacuum line seal for degassing. The samples were gently degassed with nitrogen for 15 min and then irradiated. Absorbance and fluorescence spectra were taken at intervals through the procedure above, using a Cary Bio-50 UV–vis spectrophotometer and a Varian Eclipse fluorimeter. After photolysis, the QDs were left to equilibrate for 1 h, which usually resulted in further spectral changes. Air was then allowed back into the cell to discharge excess electrons from the QDs. Transmission electron microscopy (TEM) samples were prepared by placing a drop of solution onto wax film and then placing a carbon-coated copper grid carbon side down onto the drop. After 20 s, the grid was placed on damp filter paper and left to dry in a glovebox. TEM images were obtained using a Philips CM-12 TEM equipped with an EDS analyzer for determination of the elemental composition of single particles. The images were captured with a slow scan digital camera (Gatan) and then filtered and processed using commercial image processing software (NIH Image, Adobe Photoshop).

Results

Illumination of ZnO QDs. Room-temperature hydrolysis of zinc acetate with TMAOH produces 5 nm ZnO particles which are reasonably monodisperse. The QDs are crystalline and index to wurtzite. Figure 1a shows the absorbance and fluorescence

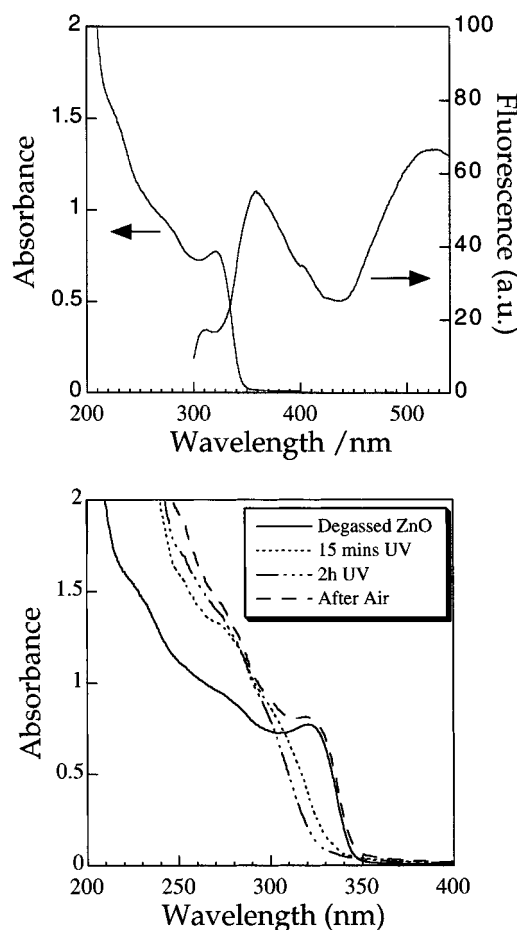
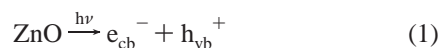


Figure 1. (a) Absorbance and fluorescence spectra of zinc oxide QDs made at 60 $^{\circ}\text{C}$, $\lambda_{\text{exc}} = 280$ nm. (b) Absorbance spectra of the ZnO QDs, shown in Figure 1a (solid line), degassed with nitrogen and irradiated for cumulative times of 15 min (dotted line) and 2 h (dashed line), and 1 h after allowing air back into the cell (dash-dot line).

spectra of the zinc oxide QD colloids used in this study. The absorption spectrum has a well-defined exciton band at 321 nm. The fluorescence spectrum has two peaks of interest, a very weak ultraviolet emission at 359 nm, which is usually attributed to direct exciton recombination,^{13,14,23} and a much broader, visible emission centered at 520 nm, which is usually attributed to the radiative recombination of free conduction electrons with trapped holes. A variety of other mechanisms have been postulated, which are reviewed by Hirschwald.²⁴ However a systematic review of the green emission by van Heusden et al.²⁵ has recently concluded that the main process is indeed recombination of a free electron and a trapped hole. The particles formed via hydrolysis with TMAOH are stable for a few days at -5°C , but the particles slowly grow over a period of hours at room temperature to about 5 nm diameter, at which point they are stable for some months. Meulenkamp and co-workers^{26,27} and Wong et al.²⁸ have shown that this process is due to Ostwald ripening.

In Figure 1b, the effects of UV irradiation of 5 nm diameter ZnO QDs are shown. The solution was degassed with nitrogen to remove dissolved oxygen. Degassing the solution had little or no effect on the absorption spectrum. After several minutes of UV irradiation, the absorption spectrum showed strong bleaching around the exciton band, as observed by numerous other groups for both ZnO colloids and ZnO electrodes.^{13,14,20} After 1 h of irradiation, the rate of formation and recombination of excited electrons had reached a steady state, and little change

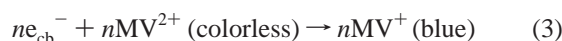
occurred in either the absorbance or the fluorescence spectrum. It is well established that the basic processes occurring in these ZnO QDs are as follows:



Excess electrons are generated on the colloid particles due to



oxidation of the organic solvent. The process is very facile. The resulting excess electrons may be trapped or mobile within the conduction band. The liberated protons from reaction 2 are likely to be adsorbed to the particle surface, due to the accumulation of excess negative charge, as a means to maintain a constant Helmholtz potential. Hole scavenging by the solvent results in electron accumulation on the QD. Eventually, a steady state is reached because holes created in the presence of existing free conduction electrons are annihilated faster than they can be scavenged by the solvent. These excess electrons can be titrated by adding an acceptor such as methyl viologen ($\epsilon_{397} = 37\,500 \text{ M}^{-1} \text{ cm}^{-1}$; $\epsilon_{602} = 12\,800 \text{ M}^{-1} \text{ cm}^{-1}$)²⁹)



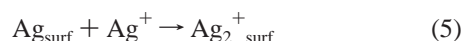
Titration of irradiated particles, which displayed exciton bleaching with MV^{2+} under careful exclusion of oxygen, demonstrated that the ZnO particles had accumulated at least 10 electrons each under steady state photolysis. This indicates that the ZnO particles are effectively degenerate and that the Fermi level after photolysis under nitrogen must lie close to the conduction band edge. Thus, there is certainly exciton bleaching of degenerate ZnO QDs. What fraction of these electrons is truly mobile and what fraction is trapped in surface states remains a moot point. The viologen titration demonstrates that the electrons transfer rapidly to a suitable acceptor in solution, so they cannot be deeply trapped in any case.

Upon standing the irradiated solution for 2–3 h, the excitonic peak slowly began to recover. This is due to slow reduction of the solvent by the excess electrons stored in the QD. These results are similar to those obtained by other groups and indicate that large numbers of electrons can be accumulated for several hours on the ZnO particles in the absence of a labile acceptor in solution or on the surface. The question now is how well this accumulated charge can be scavenged by metal islands in electrical contact with the QDs.

Silver Islands. Figure 2 shows the effects of illumination of a solution of ZnO QDs and containing $25 \mu\text{M}$ AgClO_4 . In the presence of silver ions, the excess electrons generated through reactions 1–2 now react with the metal ion to produce small metal deposits on the QD surface.



Following the initial nucleation step (reaction 4), the nascent Ag atoms scavenge further generated conduction band photoelectrons. By analogy to the photographic process, this Ag island growth is probably preceded by silver ion adsorption



After 5 min of irradiation, a surface plasmon band at 400 nm

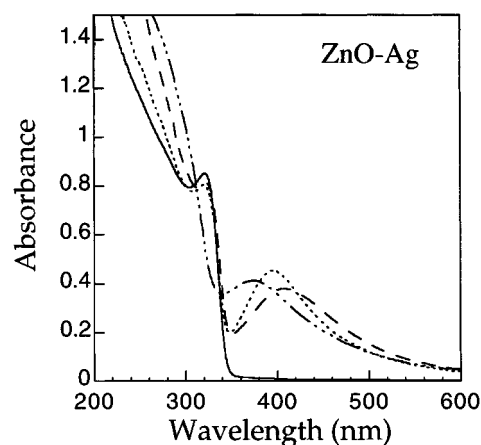
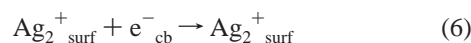


Figure 2. Absorption changes observed before (solid line) and after photolysis of 1 mM deaerated 5 nm ZnO QDs in the presence of 0.1 mM AgClO_4 in ethanol, for 15 min (dotted line) and 2 h (dotted and dashed line), and then 1 h after allowing air into the cell (dashed line).

appeared as seen in Figure 2, and the solution turned a clear yellow color. As irradiation continued, the silver plasmon band increased in intensity and blue shifted, indicating a slow increase in electron density on the silver particles.^{21,30} Throughout the first 30 min of illumination during which reduction of silver ions took place, the exciton band of the ZnO QDs remained unbleached, indicating that no excess electrons were stored on the QD while silver reduction was occurring. This is in stark contrast to the case in the absence of silver, where bleaching was observed within 5 min of illumination. After standing the colloid for an hour, the ZnO–Ag exciton band was still bleached, and the silver plasmon band was still blue shifted from its original position, so the excess electrons on the Q–ZnO and silver did not readily transfer to the solvent, ethanol. To demonstrate that both the Ag and ZnO particles had accumulated excess electrons, air was admitted back into the cell. After 2 min, the exciton peak had fully recovered, and the plasmon band had red shifted by 20 nm due to the reduction of oxygen by excess electrons on both the Ag island and the ZnO particle. The solution at this point remained a transparent yellow-brown color, and no particle coagulation was observed. Thus, both the metal and QD had been strongly cathodically polarized from the open-circuit potential in aerated ethanol.

Gold Islands. The effects of $\text{KAu}(\text{CN})_2$ reduction on the absorption spectrum of ZnO QDs are shown in Figure 3. Colloidal gold displays a surface plasmon band at 520 nm, which is ideal, since it is well removed from the region of the exciton absorption in ZnO. In this case, conduction band electrons are initially discharged via the reaction



After 5 min of irradiation, a peak at ~ 545 nm began to form, attributed to the plasmon band of gold nanoparticles.³¹ With further illumination, this peak became more intense, and blue shifted to an eventual position of ~ 520 nm. The exciton peak of Q–ZnO did not show bleaching until after 1 h of irradiation time. This suggests that either more electrons are needed to raise the Fermi energy in gold to the ZnO conduction band energy level than is the case for silver, or the gold is a better catalyst and was able to dissipate accumulated charge by electron transfer to the solvent more rapidly than silver. After standing the irradiated solution for less than 1 h, the exciton peak had fully recovered, indicating a gradual shift of excess electrons from the conduction band of zinc oxide onto the gold particles and,

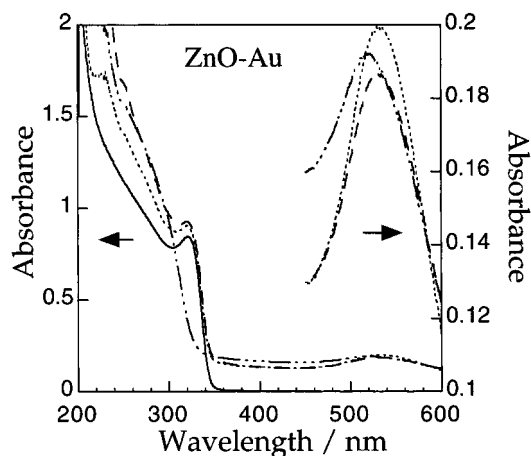


Figure 3. Absorption changes observed before (solid line) and after photolysis of 1 mM deaerated 5 nm ZnO QDs in the presence of 0.1 mM $\text{KAu}(\text{CN})_2$ in ethanol, for 15 min (dotted line) and 2 h (dotted and dashed line), and 1 h after allowing air into the cell (dashed line). The plasmon band of Au has been expanded (right-hand axis) for clarity.

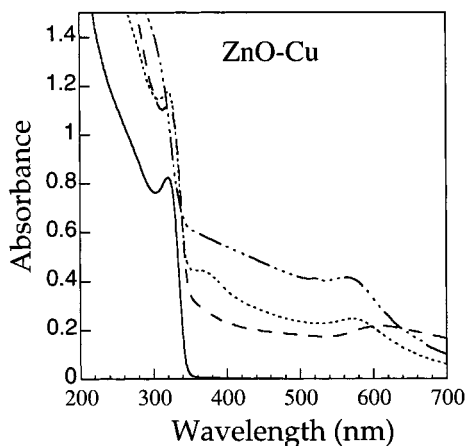


Figure 4. Absorption changes observed before (solid line) and after photolysis of 1 mM deaerated 5 nm ZnO QDs in the presence of 0.2 mM $\text{Cu}(\text{CH}_3\text{COO})_2$ in ethanol, for 15 min (dotted line) and 2 h (dotted and dashed line), and 1 h after allowing air into the cell (dashed line).

hence, into the solvent. This suggests that the main difference between gold and silver islands is in fact the rate of catalyzed ethanol reduction by the metal islands. The SP band was located at 522 nm at this point. After allowing oxygen into the solution, the position of the plasmon peak shifted immediately to 530 nm. The final color of the transparent, colloidal stable solution was a strong purple-red, due to the presence of the gold nanoparticles.

Copper Islands. The behavior of copper islands was similar to that of silver and gold. Typical results are shown in Figure 4, where 0.2 mM $\text{Cu}(\text{CH}_3\text{COO})_2 \cdot \text{H}_2\text{O}$ was added to the Q-ZnO. Addition of Cu^{2+} to Q-ZnO caused the appearance of a small peak at 370 nm due to d–d transitions in the cupric ion. Irradiation of the sample caused the appearance of a new peak at 570 nm, attributed to the plasmon band of copper metal particles. Cu nanoparticles display peaks at around 570 and 300 nm.^{31,32} As irradiation was continued, the 570 nm peak increased in intensity but, unlike gold and silver, did not concurrently blue shift during metal ion reduction. After 60 min of irradiation, the Q-ZnO exciton peak showed slight bleaching, and the copper plasmon band had blue shifted by a few nanometers. After 2 h, the Q-ZnO exciton peak was fully bleached, and the copper plasmon band was centered at 565 nm. No change was observed to the exciton band nor to the metal plasmon band on standing

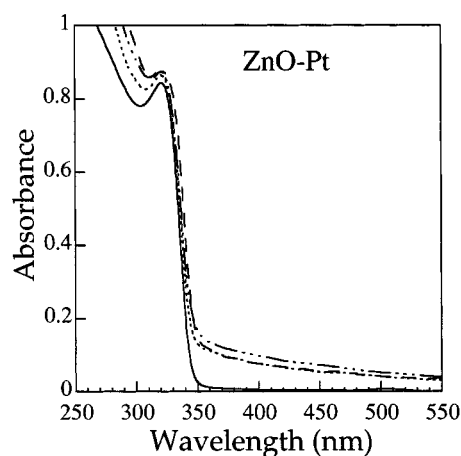


Figure 5. Absorption changes observed before (solid line) and after photolysis of 1 mM deaerated 5 nm ZnO QDs in the presence of 0.1 mM HPtCl_6^- in ethanol, for 15 min (dotted line) and 2 h (dotted and dashed line), and 1 h after allowing air into the cell (dashed line).

under nitrogen for several hours, indicating negligible rates of electron transfer to the metal from the QD and from the metal to the solvent. When air was admitted, the exciton peak recovered instantly, and the copper band red-shifted to a final position at 582 nm.

Pt Islands. The most potent hydrogenation catalysts are the Pt group metals, Pt, Pd, and Ir.³³ Unfortunately, unlike the coinage metals, Ag, Au, and Cu, these and most other transition metals do not display strong plasmon bands in the UV–visible region. This is due to the damping effect of the d–d transitions in these metals, which tend to wash out the free electron contribution to the dielectric function.²¹ As nanoparticles, these metals are normally a yellow-brown color due to the d–d transitions, and their absorption spectra are largely featureless. In Figure 5, the results of an experiment are shown in which 0.9 mM ZnO QDs were irradiated in the presence of 50 μM H_2PtCl_6 . After 5 min of UV irradiation, a ‘tail’ began to develop in the ZnO spectrum due to the formation of platinum islands. As irradiation continued, the platinum band increased in intensity, but the exciton peak of Q-ZnO showed no bleaching. In fact, even after extensive photolysis for several hours, no bleaching of the exciton band was observed. Upon admission of air, no significant change to the spectrum of the ZnO was observed.

After photodeposition, small dark patches could be observed on the ZnO particles by high-resolution electron microscopy. It was difficult to resolve the islands well enough to get accurate sizing. Figure 6 shows a high-resolution image of ZnO–Pt particles. Despite some clumping of the particles, the two types of crystal are readily resolved by electron diffraction. The inset power spectrum shows spots belonging to Pt islands with the typical fcc structure of bulk Pt. Also evident are spots which can only be indexed to the ZnO (002) reflex. The identity of both island and ZnO particles was confirmed by EDAX analysis.

Discussion

The results presented here all indicate that during photocatalysis, a QD–metal nanojunction is not necessarily as efficient a catalyst for electron discharge as may be initially envisaged. Despite the fact that the empty conduction band energy levels of all the metals lie at least 0.5–1.0 V below the ZnO conduction band, sufficient charge accumulates on the metal islands of Cu, Ag, and Au to ensure Fermi level equilibration between the QD and metal. In fact, it takes some hours for

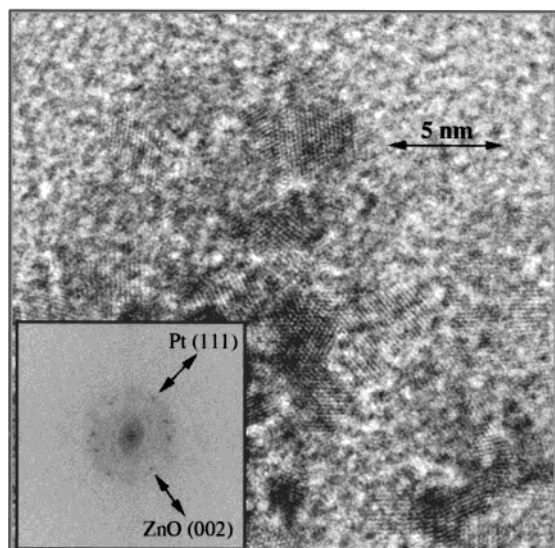


Figure 6. High-resolution TEM image of the surface of coated ZnO–Pt QDs. The Pt deposits are about 1.5–2 nm in size and are darker than the ZnO particles due to the higher electron scattering cross section of Pt. In the image, we can see two sets of lattice planes. In the power spectrum (inset), we can distinguish two sets of points, which we assign to Pt(111) and ZnO(002).

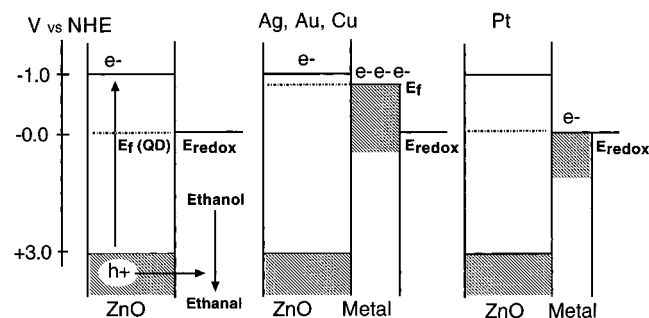


Figure 7. Scheme of the energy levels in photoirradiated ZnO QD–metal nanojunctions. (left) UV irradiation of ZnO in ethanol produces electron–hole pairs. The hole is rapidly scavenged by the solvent, leading to excess electron accumulation on the particles and exciton bleaching. The particles are degenerate after extensive photolysis in the absence of air. (middle) In the presence of Ag, Au, or Cu islands, electrons accumulate and pass to the islands where they are stored, leading to the buildup of a large Helmholtz (or diffuse layer) potential difference due to slow scavenging by the solvent. The Fermi level in the metal is shifted cathodically until it merges with the QD conduction band energy level. Almost all excess electrons are on the metal island. Both exciton bleaching and a surface plasmon blue shift are observed. (right) In the presence of Pt, rapid transfer of electrons from the Pt to the solvent occurs. The metal Fermi energy remains close to the solution redox level, and the QD Fermi energy remains in the mid-gap region. No bleaching of the exciton during photolysis is observed, and no electrons reside on the QD during photolysis.

electrons to discharge from ZnO–Ag nanoparticles in deaerated ethanol. Conversely, for ZnO–Pt at least, the Fermi level under identical photolysis conditions does not reach the conduction band of ZnO QDs. This interpretation is qualitatively summarized in Figure 7. The Fermi level in an open-circuit QD is ill-defined but will be in the midgap region (left diagram), and in principle, its position is dictated by the most facile redox couple present in solution (dotted line). The QD will contain no electrons in the conduction band. Illumination leads to electron accumulation, and the Fermi level moves up toward the conduction band energy level. Some movement of the band edges with respect to the solvent may occur, depending on the way counterions neutralize the electron density within the QD.

This is ignored in the left-hand side of Figure 7. The excess electrons are slowly discharged by the solvent over hours once photolysis and hole scavenging cease.

In the case of ZnO–metal nanojunctions, the situation is more complex. The spectral changes to the surface plasmon band of the ZnO–Ag, ZnO–Au, and ZnO–Cu particles indicate substantial electron accumulation on the metal islands during photolysis. The basic shifts that occur can be understood by considering the case of silver. Once the silver ions are completely reduced, the Fermi level in the Ag island still lies well within the band gap, probably close to +0.15 V versus NHE, its open-circuit value in water.³⁰ As the UV-irradiation continues, electronic charge flows to the Ag islands, causing a slow increase in the Fermi energy (i.e., inducing a more negative redox potential through an accumulation of excess electrons on the silver islands). The conduction band of bulk ZnO (in water) is located at least -0.8 V above the silver Fermi level.^{1,33} Yet after continuous illumination for 2 h, the zinc oxide exciton absorption band does bleach, indicating that electrons are being stored on the QD and no longer being transferred to the metal island. Weller and Hoyer found that the onset for exciton bleaching of a ZnO electrode was around -0.6 V versus NHE.²⁰ For the smaller ZnO particles used in this study, the redox potential for electrons in degenerate particles will be about 200 mV more negative than this due to size quantization effects on the energy levels. Electron transfer will cease once the silver Fermi level coincides with the ZnO conduction band edge. Hence, the Fermi level of the Ag island must have been cathodically polarized by at least -0.8 V from its typical open-circuit value in water. This condition is attained when both exciton bleaching and a strong plasmon band blue shift are observed. Consistent with this enormous polarization, the silver plasmon band peak position was located at 374 nm, which is a much shorter wavelength than normally encountered in aqueous solution (378–385 nm) even under strongly reducing conditions.²¹ This strong blue shift is only possible if silver is a very poor catalyst for ethanol reduction.

The large potential difference, which drives the metal Fermi level up until equilibration with the ZnO is achieved, is due to charging of the metal Helmholtz and diffuse double layers (see Figure 11, ref 4). The maximum Helmholtz potential difference achievable is given approximately by

$$V_H = E_{cb} - E_{redox} \quad (8)$$

It is important to recognize that the excess electron density is stored overwhelmingly on the metal islands because the Helmholtz capacitance of the metal–solution interface is much higher than the space charge capacity of the QD, even under accumulation. Hence, the Fermi level within the QD will remain near the bottom of the conduction band. Additionally, as long as only a few electrons reside on the QD, there will not be a significant shift in the position of the band edges of the QD. Slow discharge of the metal electronic charge by the solution redox couple once photolysis ceases gradually brings the Fermi levels in the metal and in the QD back to their original positions. For Ag, this takes some hours if oxygen is not present. Electron scavenging by oxygen is rapid and depletes both sides of the nanojunction in seconds.

Chen et al. previously carried out an investigation of the ZnO–Ag colloid system.^{34,35} Our observations are similar to theirs for this system. However, they concluded that the changes in the silver SP band were due to the conversion of Ag₂O islands into Ag. We believe the effects are more easily explained in terms of the Ag island electron density. The study by Ung et

al. unambiguously demonstrated that the Fermi level in silver colloids determines the position of the surface plasmon absorption band and that the shift can be quantitatively related to the effect of the excess electron density on the plasma frequency.³⁰

For Pt islands, electrons on the metal island are transferred rapidly to the solvent and the metal Fermi level remains pinned at close to E_{redox} (Figure 7 right diagram). This means there is always a strong driving force for electron transfer to the Pt from the ZnO, and few electrons accumulate during photolysis on the QD. No exciton bleaching occurs.

The number of electrons needed to be accumulated to raise the Fermi level is not easily measurable. Using spectroelectrochemistry, a double-layer capacitance of $80 \mu\text{F}/\text{cm}^2$ has been measured for Ag colloids in aqueous solution.³⁰ This value is likely to be very sensitive to particle size, solvent polarity, and dielectric perturbations due to the junction with the QD. Assuming that the double-layer capacitance of the Ag island attached to the ZnO is similar to that of the isolated Ag nanoparticles in solution, the position of the plasmon band position at 374 nm, when ZnO bleaching is seen, corresponds to a redox potential of about -0.9 V versus NHE, and to the storage of >50 electrons if the island radius is 1 nm. This corresponds very closely to the estimated position of the ZnO conduction band and confirms the fundamental result of this study, that there is equilibration of the metal and QD Fermi levels under photolysis. In fact, such blue-shifted surface plasmon bands are rarely observed for silver particles in water, and this further suggests that electron transfer from silver particles to ethanol is intrinsically slower than in aqueous media.

Conclusions

The primary aim of this initial study was to demonstrate that electron equilibration occurs in QD–metal colloid systems during photolysis. It was shown that simple spectroscopic methods enable one to monitor electron transfer processes at metal–QD junctions relatively easily. It was also demonstrated that during extensive photolysis, electron capture by metal islands of Ag, Au, and Cu becomes inhibited as the redox potential is cathodically shifted and approaches the ZnO conduction band level. At this point, electrons reside for long periods on both the QD and metal island. Photocatalysis is consequently retarded by the subsequent, rapid hole capture in the degenerate ZnO particle. Pt conversely appears to be an efficient electron sink, and virtually no electrons reside on the QD of a ZnO–Pt particle even during extended photolysis.

Acknowledgment. The authors thank the ARC for support of this research. A.W. is the recipient of a Melbourne Research Scholarship. P.M. thanks the Humboldt Foundation for support of part of this project.

References and Notes

- (1) Grätzel, M. *Heterogeneous Photochemical Electron Transfer*; CRC Press: Boca Raton, FL, 1989.
- (2) Nosaka, Y.; Ishizuka, Y.; Miyama, H. *Ber. Bunsen-Ges. Phys. Chem.* **1986**, *90*, 1199–1204.
- (3) Chandrasekharan, N.; Kamat, P. V. *J. Phys. Chem. B* **2000**, *104*, 10851–10857.
- (4) Nakato, Y.; Ueda, K.; Yano, H.; Tsubomura, H. *J. Phys. Chem.* **1988**, *92*, 2316–2324.
- (5) Nakato, Y.; Shioji, M.; Tsubomura, H. *Chem. Phys. Lett.* **1982**, *90*, 453–456.
- (6) Hiesgen, R.; Meissner, D. *J. Phys. Chem. B* **1998**, *102*, 6549–6557.
- (7) Curran, J. S.; Lamouche, D. *J. Phys. Chem.* **1983**, *87*, 5405–5411.
- (8) Gerischer, H. *J. Phys. Chem.* **1984**, *88*, 6096–6097.
- (9) Hilgendorf, M.; Spanhel, L.; Rothenhauser, C.; Muller, G. *J. Electrochem. Soc.* **1998**, *145*, 3632.
- (10) Rabani, J.; Behar, D. *J. Phys. Chem.* **1989**, *93*, 2559–2563.
- (11) Kamat, P. V.; Patrick, B. *J. Phys. Chem.* **1992**, *96*, 6829–6834.
- (12) Cavaleri, J. J.; Skinner, D. E.; Colombo, D. P., Jr.; Bowman, R. M. *J. Chem. Phys.* **1995**, *103*, 5378.
- (13) Haase, M.; Weller, H.; Henglein, A. *J. Phys. Chem.* **1988**, *92*, 482–487.
- (14) Hoyer, P.; Weller, H. *Chemical Physics Lett.* **1994**, *221*, 379–384.
- (15) Burstein, E. *Phys. Rev.* **1954**, *93*, 632.
- (16) Hilinski, E. F.; Lucas, P. A.; Wang, Y. *J. Chem. Phys.* **1988**, *89*, 3435–3441.
- (17) Colvin, V. L.; Cunningham, K. L.; Alivisatos, A. P. *J. Chem. Phys.* **1994**, *101*, 7122–7138.
- (18) Sarany, A.; Gao, R.; Rabani, J. *J. Phys. Chem. B* **2000**, *104*, 5848–5853.
- (19) Hoyer, P.; Eichberger, R.; Weller, H. *Ber. Bunsen-Ges. Phys. Chem.* **1993**, *97*, 630.
- (20) Hoyer, P.; Weller, H. *J. Phys. Chem.* **1995**, *99*, 14096–14100.
- (21) Mulvaney, P. *Langmuir* **1996**, *12*, 788–801.
- (22) Spanhel, L.; Anderson, M. A. *J. Am. Chem. Soc.* **1991**, *113*, 2826–2833.
- (23) Bahnemann, D. W.; Kormann, C.; Hoffmann, M. R. *J. Phys. Chem.* **1987**, *91*, 3789–3798.
- (24) Hirschwald, W.; Bonasewicz, P.; Ernst, L.; Grade, M.; Hofmann, D.; Krebs, S.; Littbarski, R.; Neumann, G.; Grunze, M.; Kolb, D.; Schulz, H. *Zinc Oxide: Properties and behaviour of the bulk, the solid/vacuum and solid/gas interface*; North-Holland Publishing Company: Amsterdam, 1981; Vol. 7.
- (25) Vanheusden, K.; Seager, C. H.; Warren, W. L.; Tallant, D. R.; Caruso, J.; Hampden-Smith, M. J.; Kodas, T. T. *J. Lumin.* **1997**, *75*, 11–16.
- (26) Meulenkamp, E. A. *J. Phys. Chem. B* **1998**, *102*, 5566–5572.
- (27) Meulenkamp, E. A. *J. Phys. Chem. B* **1998**, *102*, 7764–7769.
- (28) Wong, E. M.; Bonevich, J. E.; Searson, P. C. *J. Phys. Chem. B* **1998**, *102*, 7770–7775.
- (29) Bird, C. L.; Kuhn, A. T. *Chem. Soc. Rev.* **1981**, *10*, 49–82.
- (30) Ung, T.; Dunstan, D.; Giersig, M.; Mulvaney, P. *Langmuir* **1997**, *13*, 1773–1782.
- (31) Creighton, J. A.; Eadon, D. G. *J. Chem. Soc., Faraday Trans.* **1991**, *87*, 3881.
- (32) Sosebee, T.; Giersig, M.; Holzwarth, A.; Mulvaney, P. *Ber. Bunsen-Ges. Phys. Chem.* **1995**, *99*, 40–49.
- (33) Bockris, J. O. M.; Khan, S. U. M. *Surface Electrochemistry*; Plenum Press: New York, 1993.
- (34) Chen, S.; Nickel, U. *J. Chem. Soc., Chem. Commun.* **1996**, 133–4.
- (35) Chen, S.; Nickel, U.; Ren, X. *J. Colloid Interface Sci.* **1995**, *176*, 286–92.